INTERNATIONAL JOURNAL OF MECHANICAL ENGINEERING AND TECHNOLOGY (IJMET)

ISSN 0976 – 6340 (Print)
ISSN 0976 – 6359 (Online)
Volume 4, Issue 3, May - June (2013), pp. 244-258
© IAEME: www.iaeme.com/ijmet.asp
Journal Impact Factor (2013): 5.7731 (Calculated by GISI)
www.jifactor.com

IJMET
© I A E M E

MEASUREMENT OF DEVOLATILIZATION TIME AND TRANSIENT SHRINKAGE OF A CYLINDRICAL WOOD PARTICLE IN A BUBBLING FLUIDIZED BED COMBUSTOR

M. Sreekanth

School of Mechanical and Building Sciences, VIT University, Chennai Campus, Vandalur - Kelambakkam Road, Chennai - 600 127, India.

ABSTRACT

This work presents the results of experiments conducted to determine the mass loss and size reduction characteristics of a cylindrical wood particle undergoing devolatilization under oxidation conditions in a bubbling fluidized bed combustor. Cylindrical wood particles having five different sizes ranging from 10 to 30 mm and aspect ratio (*l*/*d*=1) have been used for the study. Experiments were conducted in a lab scale bubbling fluidized bed combustor having silica sand as the inert bed material and air as the fluidizing medium. Devolatilization time, and radial and longitudinal shrinkages have been measured during and at the end of devolatilization. Studies have been carried out at three different bed temperatures (T_{bed}=750, 850 and 950 °C), two inert bed material sizes (mean size d_p=375 and 550 µm) and two fluidizing velocities ($u=5u_{mf}$ and $u=10u_{mf}$). Devolatilization time is most influenced by the initial wood size and bed temperature. Longitudinal shrinkage begins after 50% of conversion while radial shrinkage occurs right from the beginning. There was no clear influence of the fluidization velocity and bed particle size on the parameters studied.

Key words: Wood; Devolatilization; Fluidized bed; Shrinkage.

1. INTRODUCTION

Devolatilization is an important stage of wood combustion, due to the amount of volatiles contained in it (~ 75% by mass) and the amount of heat contained in them (~ 80% by mass). The rate of devolatilization determines the speed at which the volatiles release, depending on which the type of feeding to the bed (under feeding or over feeding) and

location of the feed points could be established. Therefore physical changes that take place in the wood particle during devolatilization need to be studied.

Wood is known to shrink during devolatilization. It is also known to fragment under certain combustor conditions[1-3]. Both these phenomena greatly reduce the size of the wood particle. The reduced size could have significant influence on the heat conducted and oxygen diffusion into the particle and on the rate of the subsequent chemical reactions. Significant size reduction could result in elutriation of un-burnt fuel, thereby causing direct carbon loss. The size reduction could also play a dominant role in the sizing of the down-stream particulate collection equipment.

A number of published articles report experimental investigations of devolatilization time and final char yield of wood in different types of combustors and under different conditions[4]. Shrinkage of millimeter sized wood under fluidized bed combustor conditions have been reported by [5]. But they have measured shrinkage at the end of devolatilization. All the devolatilization models assume that shrinkage depends linearly on the degree of conversion, which may not be true. Davidsson *et al.* [6] reported time dependant (Transient) shrinkage measurement of 5 mm cubes in a single particle reactor, where they noticed that the shrinkage is not linear. Such measurements have not been reported under fluidized bed combustion conditions. Fluidized beds have low carbon loading and high heat transfer coefficients when compared to single particle reactors. Also, in a fluidized bed, the atmosphere is oxidizing while that in the above mentioned single particle reactor is nitrogen.

Therefore the present work aims at studying the Devolatilization Time (τ_d) and Shrinkage at different operating conditions. For a wider range of applicability, experiments are conducted at different wood particle sizes, bed temperatures, inert bed material sizes and fluidization velocities.

2. EXPERIMENTAL

All the experiments were conducted in a laboratory-scale bubbling fluidized bed combustor. A schematic diagram of the experimental facility is shown in Figure 1. The combustor mainly consists of a stainless steel reactor, the diameter of which is 130 mm and the height is 600 mm. The reactor is provided with silicon carbide heaters close to its outer surface to maintain the bed temperature at a desired value. The inert bed material is supported by a distributor plate, and the static bed height is kept same as the reactor diameter. The pre-heated air necessary for fluidizing the bed is supplied by a blower before being heated to 200 °C by air pre-heaters. The air quickly assumes the bed temperature on entering it due to the good mixing and high heat transfer rates prevalent in the bed. This was in return verified by the temperatures measured at different heights of the bed. Tables 1 and 2 give the experimental details.

The fuel wood, *Casuarina Equisetifolia* in this case, was de-barked and turned on a lathe to the required dimensions. The centre of the branch was coinciding with the axis of the cylinder. Prior to each experiment, every wood sample was weighed and its dimensions noted. Also, one sample from each batch of wood samples was dried in a moisture balance to determine the amount of moisture contained. This moisture content was attributed to all the samples in the batch and this sample was never used in the experiments. The moisture contained in the wood varied from 7 to 22 % during the experimental campaign. The proximate and ultimate analyses of Casuarina Equisetifolia are given in Table 3.

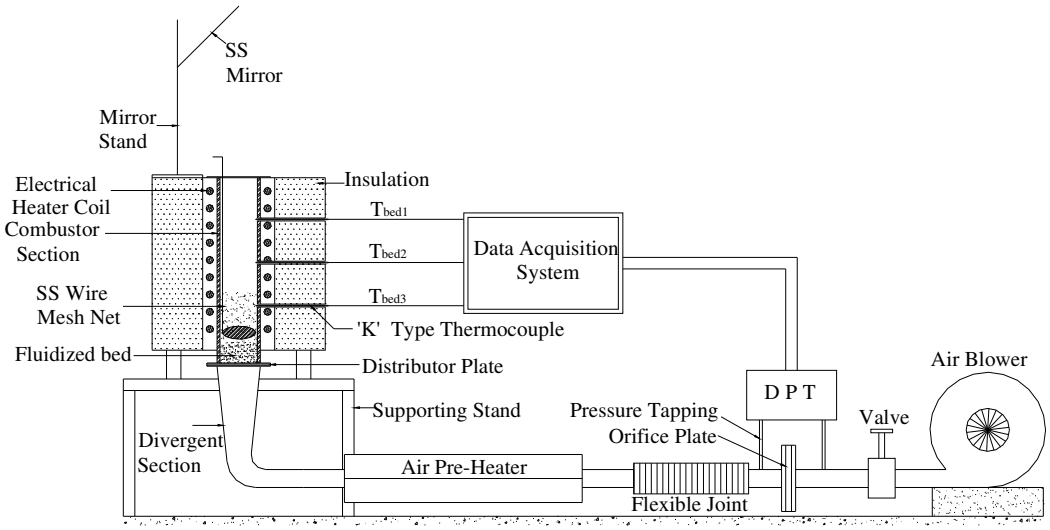

Figure 1: Schematic diagram of the bubbling fluidized bed combustor setup

Table 1: Experimental conditions

Reactor material	316 grade stainless steel
Reactor diameter	130 mm
Reactor height	600 mm
Static bed height	130 mm
Bed temperature	750, 850, 950 °C
Inert bed material	Silica sand, 375, 550 µm
Pre-heated air temperature	200 °C
Fluidizing velocity	$u=5u_{mf}$, $10u_{mf}$
Fuel shape	Cylinder
Fuel size (*l/d*)	10/10, 15/15, 20/20, 25/25, 30/30 mm

Table 2: Fluidizing velocities

Bed temperature (°C)	d_p=375 µm		d_p=550 µm	
	$5u_{mf}$ (m/s)	$10u_{mf}$ (m/s)	$5u_{mf}$ (m/s)	$10u_{mf}$ (m/s)
750	0.25	0.5	0.54	1.1
850	0.24	0.48	0.51	1
950	0.22	0.45	0.48	0.96

Table 3: Proximate and Ultimate analysis of *Casuarina Equisetifolia*

Quantity	Content (%)
Proximate Analysis	
Moisture	10.8
Volatiles	72.5
Fixed carbon	16.4
Ash	0.3
Ultimate Analysis	
Carbon	42.5
Hydrogen	6.1
Nitrogen	0.16
Oxygen	51.24

The experimental procedure is described below. Once the combustor conditions have been established, a wood particle of known mass and size was introduced into the bed with the help of a stainless steel basket. The basket was made up of a stainless steel mesh (304 grade) having an opening approximately equal to twice the bed material size, in order to facilitate free flow of the material in and out of the basket and also to minimize the char loss to the bed. The basket diameter is 110 mm, which leaves enough clearance between itself and the thermocouples protruding from the sides of the reactor. The basket is 200 mm tall so that the fuel particle does not escape from the top due to bed expansion. The basket along with the wood particle is pushed into the bed until it touches the bottom. The fuel particle ignites on entering the bed and begins to move chaotically along with the sand inside the basket. Most of the time, volatiles' flame was seen on top of the bed along with the fuel particle. The end of devolatilization was inferred by the extinguishing of the flame. The time elapsed between the introduction to the flame extinction (Flame extinction time, FET) was noted. The char particle(s) remaining at the end of devolatilization were taken out of the bed with the basket and immediately quenched using fine sand (375 μm) at room temperature. The time elapsed between removal and complete quenching was about 4 seconds. On cooling, the char particles were carefully separated from the sand and their dimensions measured. This procedure was repeated five times to establish an average devolatilization time. The average devolatilization time (τ_d) is then divided into four equal parts. A fresh wood particle was then subjected to devolatilization for a period of 1/4 τ_d and removed immediately, quenched, cooled, counted and measured for dimensions. This procedure was repeated three times for each quarter of τ_d. The entire experiment therefore needs 14 samples and takes about one hour for completion. After completion the char samples were preserved in labeled air-tight plastic pouches.

3. RESULTS AND DISCUSSION

3.1. Devolatilization time (τ_d)

3.1.1. Influence of size and bed temperature

Devolatilization of large particles which are used in fluidized bed combustors is mainly heat transfer controlled. Also, the devolatilization is known to take place within a temperature window of 350 - 600 ^{0}C. The speed at which the heat wave penetrates through

the particle determines the devolatilization time. Figure 2 shows the devolatilization times obtained at the three bed temperatures under study. It can be seen that devolatilization time is longer at lower bed temperatures and for larger wood particles.

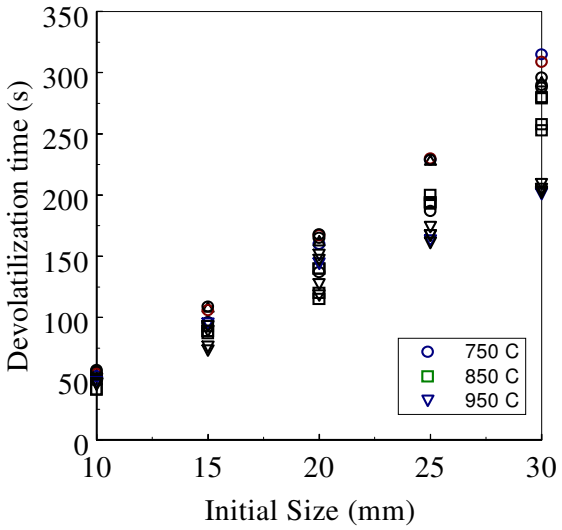

Figure 2: Devolatilization time of cylinders at different bed temperatures and inert bed material size of dp=375 µm, u=5umf

3.1.2. Influence of fluidization velocity

The influence of the fluidization velocity at 850 and 950 °C on the devolatilization time is shown in Figure 3(a) and 3(b) respectively. There appears to be no definite influence of the fluidization velocity on the devolatilization time. This could be due to the fact that increased velocity increases the surface heat transfer rate but the conduction resistance within the particle is quite dominant, thereby nullifying the effects at the surface. The deviations in the devolatilization times could be attributed to the varying properties of the wood samples.

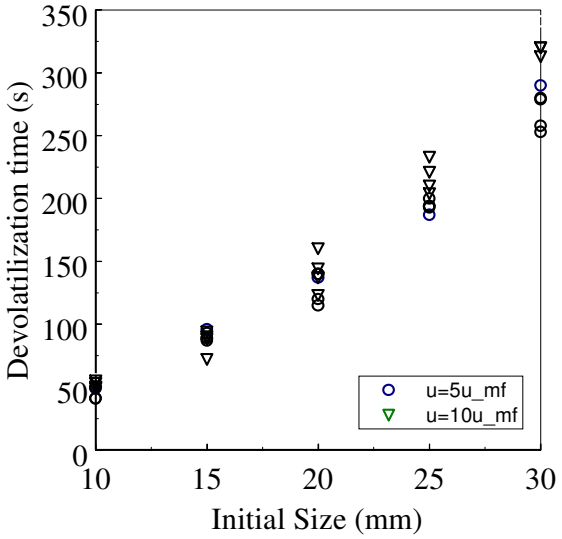

Figure 3a: Devolatilization time at two different velocities. Tbed=850 °C, dp=375 µm

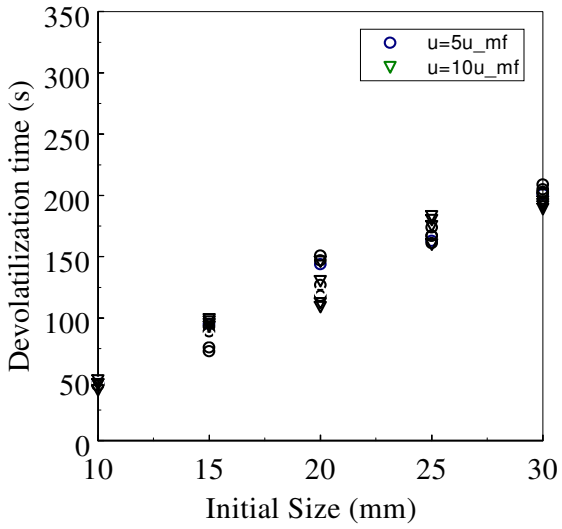

Figure 3b: Devolatilization time at two different velocities. Tbed=950 °C, dp=375 µm

3.1.3. Influence of inert bed material size

Figures 4(a) and 4(b) show the influence of different bed material size on the devolatilization time at bed temperatures of 750 and 850 °C respectively. In this case too, no definite influence of bed material was seen except in Figure 4b, for the 30/30 mm particle, the 550 µm bed particle results in a lower devolatilization time than the 375 µm bed particle. More over, any difference was noticeable only for the larger wood particles.

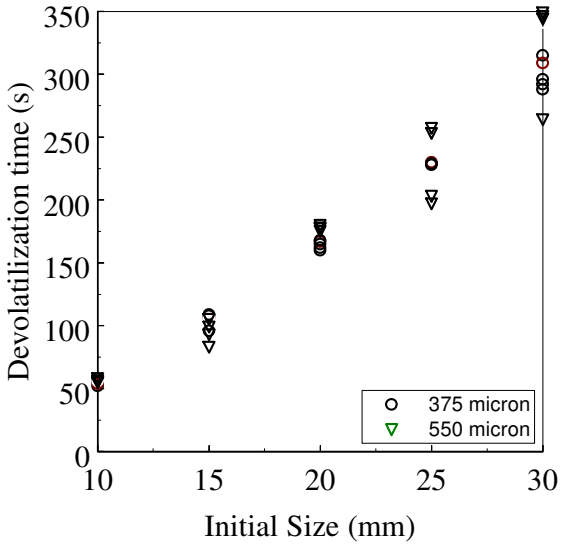

Figure 4a: Devolatilization time at different inert bed material sizes. Tbed=750 °C, u=5umf

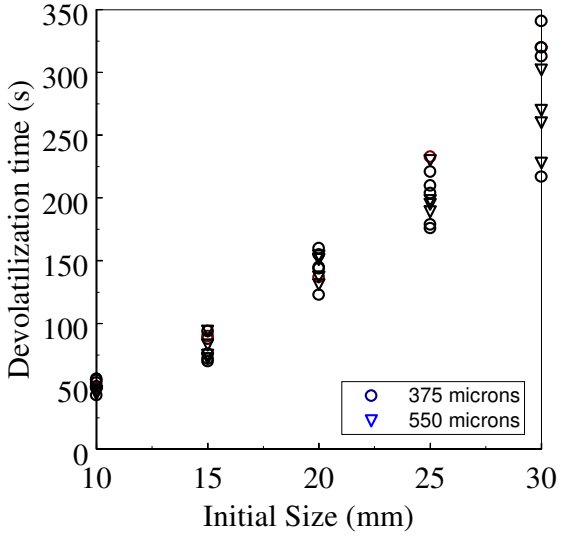

Figure 4b: Devolatilization time at different inert bed material sizes. Tbed=850 °C, u=10umf

All the data obtained for the devolatilization time at different bed temperatures, inert bed material sizes and velocities was used to obtain a correlation for the devolatilization time. The correlation is given in the form:

$$\tau_d = a d_{cyl}^{b} T_{bed}^{-c}$$

The present correlation predicts the present experimental devolatilization times with a maximum error of 16%, while Renu *et al*[4]. correlation had a maximum deviation of 13%. But their experiments were conducted at a single velocity and for one size of bed material. The correlation obtained for the present work is given as:

$$\tau_d = 248 d^{1.646} T_{bed}^{-0.78} \pm 16\%$$

In the above correlation, the time is measured in seconds, diameter in mm and bed temperature in Kelvin.

3.2. Shrinkage

Shrinkage is the reduction in the size of the wood particle during devolatilization and it can be defined by the ratio of instantaneous size reduction to the initial size. Mathematically it can be represented as:

$$\text{Shrinkage} = \frac{\text{Reduction in dimension}}{\text{Initial dimension}} \times 100$$

Shrinkage can be measured in the longitudinal and radial directions for a cylindrical wood particle and the volumetric shrinkage can be computed from this measured data.

3.2.1. Longitudinal shrinkage

3.2.1.1. Influence of size

Figure 5 shows the longitudinal shrinkage of cylindrical wood particles at different sizes and temperatures. To obtain an overall view, the shrinkage values obtained at different bed particle sizes and velocities have been used in the plot. It can be seen that there is a decrease in the longitudinal shrinkage as the size increases. This could be due to decreasing amount of heat transferred in the longitudinal direction as the particle length increases. The shrinkage ranges from 7-25 %. There is no clear influence of the temperature visible on the longitudinal shrinkage, from this graph.

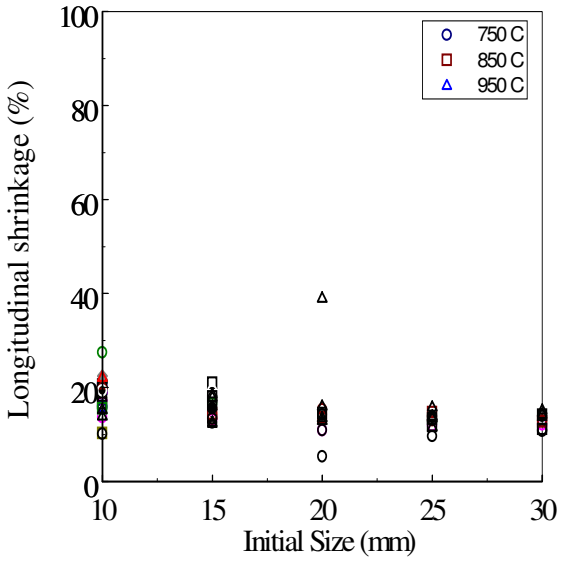

Figure 5: Influence of size on the longitudinal shrinkage

3.2.1.2. Influence of bed temperature

Figure 6 shows the longitudinal shrinkage in a 10/10 mm wooden cylinder devolatilized at different bed temperatures. It can be seen that the shrinkage increases with a rise in the bed temperature. This again can be explained by the increased rate of heat transferred due to a rise in the bed temperature. Therefore, for the particle sizes considered, the rate of heating and therefore the surrounding temperature appears to slightly influence the amount of lengthwise shrinkage.

The correlation for Longitudinal Shrinkage (s_l) is given as:

$$s_l = -0.295d + 20.7 \pm 8\%$$

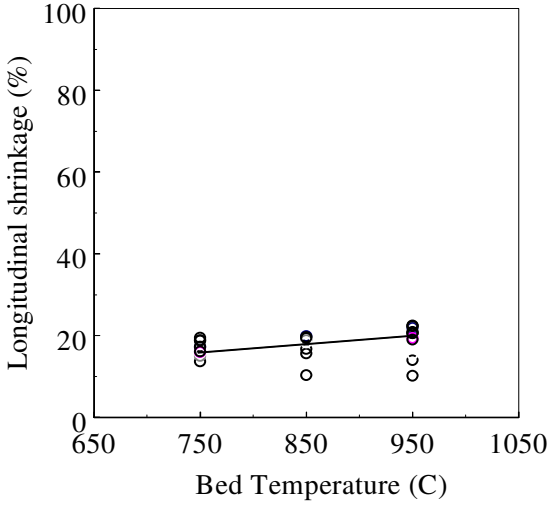

Figure 6: Influence of bed temperature on the longitudinal shrinkage of a 10/10 mm cylinder

3.2.1.3. Variation with degree of conversion

The degree of conversion is defined as:

$$\text{Degree of conversion} = \left[1 - \frac{\text{Instantaneous mass}}{\text{Initial dry mass}}\right] \times 100$$

Figure 7 shows the variation of the longitudinal shrinkage with the degree of conversion obtained at a bed temperature of 950 °C. To obtain an overall view, all the data points for various wood sizes, bed particle sizes and velocities are included. The graph shows that very little shrinkage takes place till a conversion of 50% was achieved. This implies that the wood constituents along the length begin to decompose only at the later stages of devolatilization. It can also be seen that the longitudinal shrinkage increases linearly until the degree of conversion attains a value of 75%. Beyond that, in the last stage of conversion, there is a steep rise in the longitudinal shrinkage.

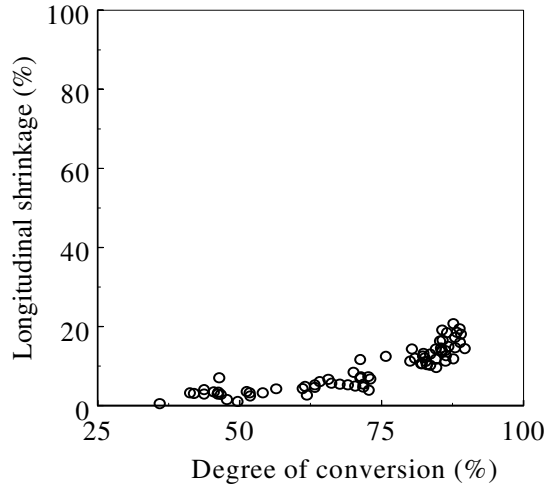

Figure 7: Variation of longitudinal shrinkage with the degree of conversion. Tbed=950 °C

3.2.2. Radial shrinkage

3.2.2.1. Influence of size

Figure 8 shows the variation of radial shrinkage with the size. To obtain an overall view, the shrinkage values obtained at different bed particle sizes and velocities have been used in the plot. For the size 30/30 mm, only few data points were available as most samples fragmented. The radial shrinkage ranges from 10% to 35%. It can be seen that there is a slight increase in the radial shrinkage with the size but the figure gives no clear indication of the influence of temperature.

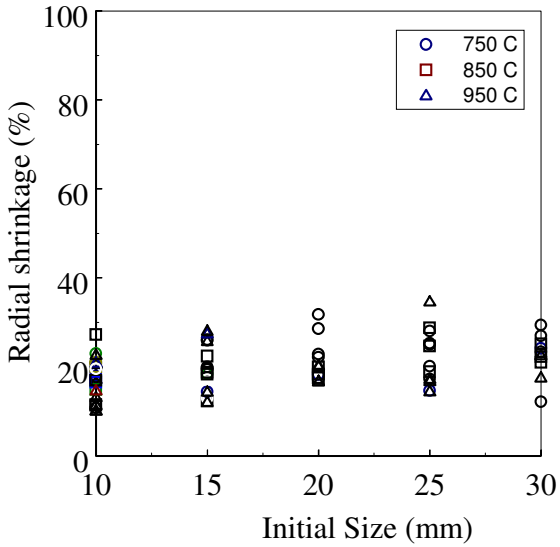

Figure 8: Influence of size on the radial shrinkage

3.2.2.2. Influence of bed temperature

Figure 9 shows the influence of bed temperature on the radial shrinkage at the end of devolatilization. It can be seen that there is a strong reduction in the amount of shrinkage as the bed temperature rises. At higher bed temperatures, when the heat transfer rate is high, the reactions causing radial shrinkage do not have enough time to proceed. Since wood comprises of different constituents (cellulose, hemi-cellulose and lignin) which react at different temperatures, this is possible.

The correlation for Radial Shrinkage (s_r) is given as:

$$s_r = 150.5 d^{0.224} T_{bed}^{0.379} \pm 17\%$$

where the bed temperature is in absolute units.

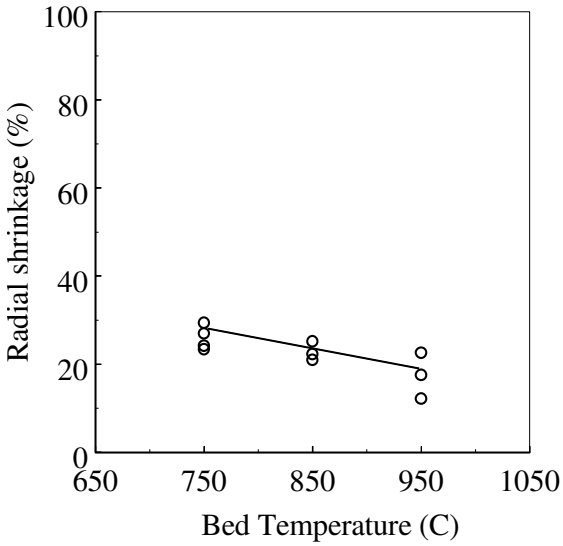

Figure 9: Influence of bed temperature on the radial shrinkage of a 30/30 mm cylinder

3.2.2.3. Variation with degree of conversion

Figure 10 shows the variation of radial shrinkage with the degree of conversion at a bed temperature of 750 °C. Radial shrinkage varies between 8 to 30%. Shrinkage begins quite early in the conversion process and then there is a steady linear rise in the shrinkage till the degree of conversion reaches 75% beyond which the shrinkage rises steeply.

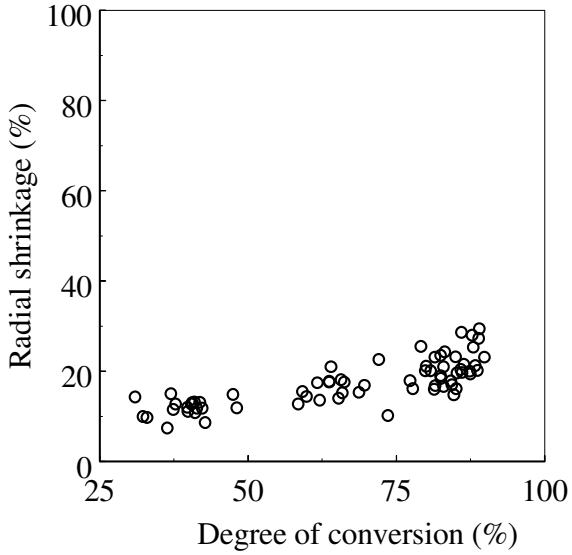

Figure 10: Variation of radial shrinkage with the degree of conversion. Tbed=750 °C

3.2.3. Volumetric shrinkage

3.2.3.1. Influence of size

Figure 11 shows the influence of size on the volumetric shrinkage. To obtain an overall view, the shrinkage values obtained at different bed particle sizes and velocities have been used in the plot. The volumetric shrinkage varies between 30 and 60 % and there was almost no influence of size on the amount of volumetric shrinkage. This could be due to decreasing longitudinal shrinkage and increasing radial shrinkage with increasing size.

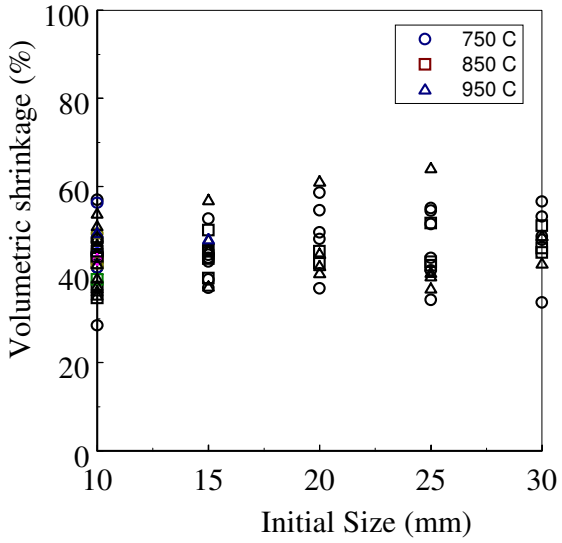

Figure 11: Influence of size on the volumetric shrinkage

3.2.3.2. Influence of bed temperature

Figure 12 shows the influence of bed temperature on the volumetric shrinkage of a 20/20 mm cylinder. The volumetric shrinkage slightly decreases with a rise in temperature. The volumetric shrinkage is computed from the longitudinal and radial shrinkages. Since it depends on the square of radial shrinkage, it has the same behaviour of that of radial shrinkage.

The correlation for Volumetric Shrinkage (s_v) is given as:

$$s_v = 23.35 d^{0.0917} T_{bed}^{0.0555} \pm 10\%$$

where the bed temperature is in absolute units.

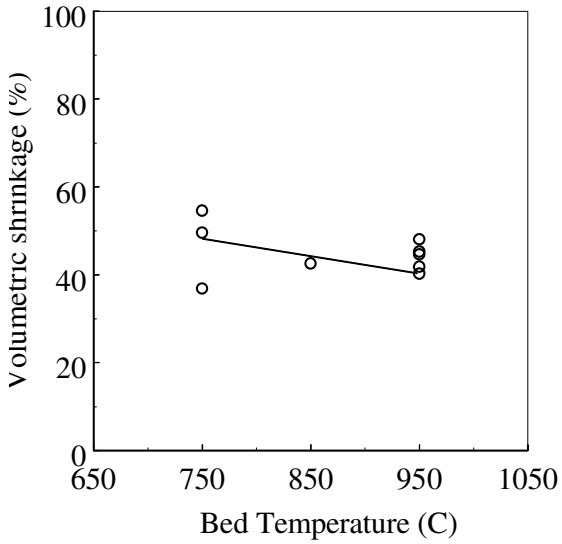

Figure 12: Influence of bed temperature on volumetric shrinkage of a 20/20 mm cylinder

3.2.3.3. Variation with degree of conversion

Figure 13 shows the variation of volumetric shrinkage with the degree of conversion at a bed temperature of 850 °C. It can be seen that up to a value of 75%, the rise is linear but steep while beyond 75%, it is non-linear and very steep. The steepness is due the influence of the radial shrinkage just mentioned.

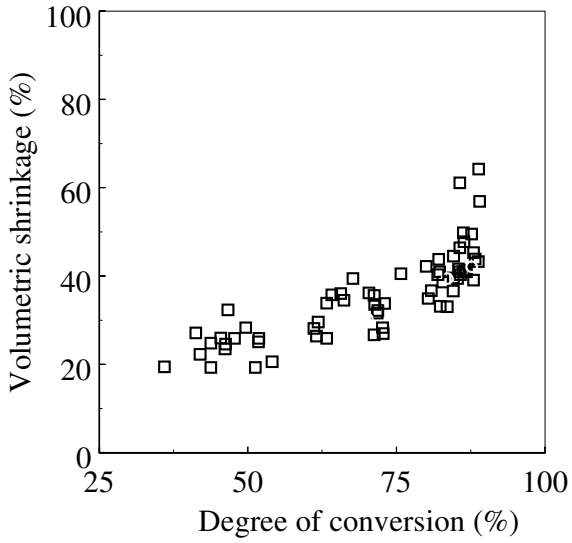

Figure 13: Variation of volumetric shrinkage with the degree of conversion. Tbed=850 °C

Figure 14 shows the longitudinal, radial and volumetric shrinkages of wooden cylinders at a bed temperature of 850 °C. It can be seen that the dependence is different from linear. As most models of devolatilization assume a linear relationship between the shrinkages and degree of conversion, in case the models are sensitive to shrinkage, they will need modifications.

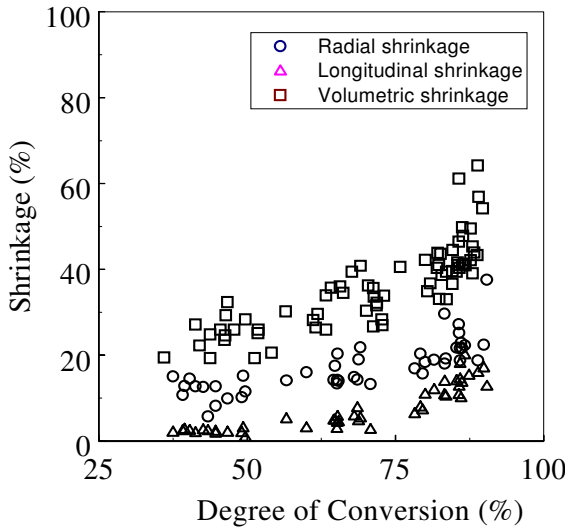

Figure 14: Shrinkage as a function of the degree of conversion. T¬bed=850 °C

Figure 15 shows the longitudinal, radial and volumetric shrinkages of all the sizes subjected to devolatilization at a bed temperature of 750 °C. Longitudinal shrinkage is steep during the second half of the devolatilization time while radial shrinkage and therefore volumetric shrinkage is fast during the initial stages and is less steep during the later stages.

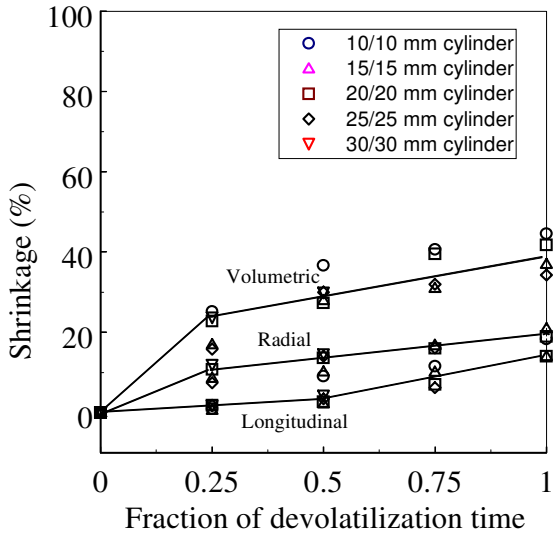

Figure 15: Progress of shrinkage during devolatilization. Tbed=750 °C

4. CONCLUSIONS

1. Devolatilization time increases with the initial wood particle size while it decreases with bed temperature.
2. The longitudinal shrinkage is independent of the bed temperature while radial shrinkage is strongly dependent on it.
3. Shrinkage does not depend linearly on the degree of conversion. Longitudinal shrinkage occurs mostly after 50% of the conversion, while radial and volumetric shrinkages occur from the beginning of the conversion process.
4. Correlations for Devolatilization Time and final Shrinkage in longitudinal and radial directions have been proposed.

ACKNOWLEDGEMENT

The reported experimental work has been carried out in the Heat Transfer and Thermal Power Laboratory at the Indian Institute of Technology Madras (IIT Madras) by the funding provided by The Swedish International Development Agency (SIDA). The author is grateful for the same.

REFERENCES

[1] Chirone, R.; Greco, G.; Salatino, P.; Scala, F. (1997) The relevance of comminution phenomena in the fluidized bed combustion of a biomass (Robinia Psuedoacacia), Proceedings of the 14th International Conference on Fluidized Bed Combustion, ASME, 145-150.
[2] Scala, F.; Chirone, R. (2004) Fluidized bed combustion of alternative solid fuels, Experimental and Thermal Fluid Science, 28(7), 691-699.
[3] Sreekanth, M.; Ajit Kumar Kolar, Leckner, B. (2006) Effect of Shape and Size of Wood on Primary Fragmentation in a Laboratory Scale Fluidized Bed Combustor, Paper No. 97, 19th International Conference on Fluidized Bed Combustion, Rutzky Druck, St. Poelten, Vienna, Austria.
[4] Renu Kumar, R; Ajit Kumar Kolar, Leckner, B. (2004) Effect of fuel particle shape and size on devolatilization time of Casuarina wood. Science in Thermal and Chemical Biomass Conversion, Vancouver Island, Victoria BC, Canada, August-September.
[5] Renu Kumar R, Ajit Kumar Kolar and Bo Leckner. (2006) Shrinkage characteristics of Casuarina wood during devolatilization in a fluidized bed combustor. Biomass & Bioenergy, 30(2),153-165.
[6] Davidsson, K.O.; Pettersson, J.B.C. (2002) Birch wood particle shrinkage during rapid pyrolysis, Fuel, 81, 263-270.
[7] Ayub A. Miraje and Dr. Sunil A. Patil, “Infinite Fatigue Life of Three Layer Shrink Fitted Compound Cylinder under Fluctuating Internal Pressure”, International Journal of Mechanical Engineering & Technology (IJMET), Volume 3, Issue 1, 2012, pp. 288 - 299, ISSN Print: 0976 – 6340, ISSN Online: 0976 – 6359.